Computers and Structures 89 (2011) 507–516

Contents lists available at ScienceDirect

Computers and Structures

journal homepage: www.elsevier.com/locate/compstruc

Analytical modeling of wave propagation in orthogonally rib-stiffened sandwich structures: Sound radiation

F.X. Xin *, T.J. Lu

MOE Key Laboratory for Strength and Vibration, School of Aerospace, Xi'an Jiaotong University, Xi'an 710049, PR China

ARTICLE INFO

Article history:
Received 19 May 2010
Accepted 6 December 2010
Available online 31 December 2010

Keywords:
Sound radiation
Wave propagation
Vibration
Sandwich structures
Rib-stiffener

ABSTRACT

Wave propagation in an infinite sandwich panel reinforced by orthogonal rib-stiffeners is theoretically formulated for harmonic point force excitation. The motions of the equally spaced rib-stiffeners are handled by considering their tensional, bending vibrations and torsional movements. The response of the sandwich is determined by employing the Fourier transform technique and considering the periodical nature of the structure, which is numerically solved by truncating two infinite sets of simultaneous equations insofar as the solution converges. The far field radiated sound pressure is examined relative to that of an unstiffened panel with useful conclusions deduced.

1. Introduction

Wave propagation and sound radiation behaviors of periodically rib-stiffened structures are of significant interest due to their increasing applications in civil and transport engineering, e.g., as the cabin skin of aircrafts, marine ships and express trains [1–20]. At low frequencies, a rib-stiffened structure can be approximated as an orthotropic panel when the panel flexural wave has a wavelength much greater than stiffener spacing [3,7]. However, at high frequencies when the wavelength is comparable with stiffener spacing, the spatial periodicity of the structure should be carefully taken into account in any theoretical modeling.

There exist a multitude of analytical studies on the vibroacoustic behavior of periodically rib-stiffened structures, including beams and plates. For example, the response of a periodically supported beam subjected to spatially and temporally harmonic pressure was solved by Mead and Pujara [21] using a particular series of space harmonics. The space-harmonic method evolving from the considerations of progressive wave propagation is superior to the classical normal mode approach, since only as few as seven terms can ensure accurate convergence of the solution. Subsequently, with emphasis placed on wave propagation characteristics, Mead and Yaman [22] developed an exact model for the harmonic response of a uniform finite beam on multiple supports. From the viewpoint of free wave propagation, Mead [23] investigated theoretically an infinite beam on regularly spaced identical supports in terms of superposed sinusoidal waves. For more details regarding wave propagation in continuous periodic structures, one may consult the review [24].

As for periodically rib-stiffened plates, a few typical works can be referred to. For instance, multi-mode wave propagation in a one-dimensionally (1D) stiffened plate was theoretically and experimentally investigated by [1,2], who also examined its energy propagation features in k-space and the corresponding dispersion relations. Using the principle of superposition, Rumerman [25] proposed a general solution for the forced vibration of an infinite thin plate, periodically stiffened by identical, uniform rib-stiffeners. An approximate method was employed by Mead and Mallik [26] to estimate the sound power radiated by an infinite plate, supported elastically along parallel, equi-spaced lines and subjected to a simple pressure field convecting uniformly over the plate. Whilst Mead and Parthan [27] studied the propagation of flexural waves in a plate resting on an orthogonal array of equi-spaced simple line supports, Mace [28] presented a solution for the radiation of sound from a point-excited infinite fluid-loaded plate reinforced by two sets of parallel stiffeners. Several aspects related to the vibration of and sound radiation from periodically line-stiffened and fluid-loaded plates were further examined by Mace [3,4]. The far- and near-field acoustic radiation of an infinite periodically rib-stiffened plate was obtained theoretically by Cray [29], although only the tensional forces of the rib-stiffeners were accounted for. Wang et al. [30] proposed a theoretical model of sound transmission across double-leaf partitions having periodical parallel rib-stiffeners using the space harmonic approach: except for the torsional moments, both the tensional forces and bending moments of the rib-stiffeners were accounted for.

* Corresponding author. Tel.: +86 29 82665600; fax: +86 29 83234781.
E-mail addresses: fengxian.xin@gmail.com (F.X. Xin), tjlu@mail.xjtu.edu.cn (T.J. Lu).

0045-7949/$ - see front matter © 2010 Elsevier Ltd. All rights reserved.
doi:10.1016/j.compstruc.2010.12.007

A few investigations also focused on the pass-/stop-band characteristics of wave propagation in periodically rib-stiffened plates. For instance, the transmission of energy in 1D periodically ribbed membrane was theoretically studied by Crighton [31] when the structure was immersed in static compressible fluid and excited by a time-harmonic line force. Later, addressing essentially the same problem, Spivack [32] gave an exact solution for general finite configurations and found that the pass-band response becomes increasingly sensitive to frequency as the length of rib array increases. A further investigation on the band structure of energy transmission in periodically ribbed elastic structures under fluid loading was carried out by Cooper and Crighton [33,34] using the Green's function method, from the viewpoint of spatial periodicity in the pass-bands and that of algebraic decay in the stop-bands, respectively.

Although the vibroacoustic behaviors of periodically rib-stiffened structures have been studied by many researchers, commonly only with the tensional forces of the rib-stiffeners considered: the influence of their bending and torsional moments as well as inertial effects remains unclear. Moreover, previous researches focused mainly on relatively simple structures, e.g., infinite periodically supported beams and 1D rib-stiffened plates. Only a noticeably few [5,6] considered the more general two-dimensional (2D) rib-stiffened structures that are of practical importance in aeronautical and marine applications. For example, Mace examined the radiation of sound from an infinite fluid-loaded plate reinforced with two sets of orthogonal line stiffeners [5], and the vibration of a thin plate lying on point supports that form an orthogonal 2D periodic array [6]. However, in the analysis [5], it was assumed that the stiffeners only exert forces on the plate.

To address the aforementioned deficiencies, we aim to study analytically the vibration and acoustic radiation of a generic 2D periodical structure that is consisted of two infinitely large parallel plates reinforced by orthogonally extended rib-stiffeners (i.e., a sandwich panel with orthogonal rib-stiffener arrays as its core). To accurately model the motion of each rib-stiffener, its tensional, bending and torsional vibrations are all considered. The inertial effects arising from the mass of the rib-stiffeners are also taken into account, by introducing the inertial terms of their tensional forces, bending moments and torsional moments into the governing equations of panel vibration. Fourier transform is employed to solve the resulting governing equations, leading to two sets of infinite algebraic equations, which are truncated to solve insofar as the solution converges. In terms of obtained panel responses, the radiated sound pressure at far field is numerically calculated to gain physical insight on wave propagation and sound radiation of the sandwich structure. Good agreements between model predictions with previous published results [5] validate the present analytic model and confirm the necessity of including the inertial effects and torsional moments of the rib-stiffeners in any theoretical modeling especially at high frequencies. The influences of inertial effects, excitation position, and spatial periodicity of rib-stiffeners on the vibroacoustic behavior of the sandwich are quantified with the underlying physical mechanisms explored.

Although this paper focuses to solve and discuss a relatively specific problem, while the theoretical model proposed can be readily employed to solve the similar problems of periodic structures. In particular, the theoretical model based on Fourier transform technique could be referential to mend finite element method so as to solve more generalized problems efficiently. For this point, Kohno et al. [35] have done an excellent job by combining the advantages of finite element method and spectral method to solve problems of wave propagation. This work should be very useful for enlightening us to extend our theoretical work for more generalized problems, for example, by combining the advantages of our theoretical model and finite element method.

2. Theoretical modeling of structural dynamic responses

2.1. Statement of problem

Consider an infinitely large 2D sandwich structure shown schematically in Fig. 1, which has a lattice core in the form of orthogonal stiffeners having periodic uniform spacings in the x- and y-directions, l_x and l_y, respectively. Its geometrical dimensions are: depth of orthogonal rib-stiffener core d, thickness of upper and bottom panels h_1 and h_2, and thickness of x- and y-wise stiffeners t_x and t_y. The mass densities of the x- and y-wise stiffeners are m_x and m_y, respectively. A right-handed Cartesian coordinate system (x,y,z) is established, with its x- and y-axes located on the surface of the upper panel and the positive direction of the z-axis pointing downward (Fig. 1).

Let a harmonic point force with amplitude q_0 be applied on the surface of the upper panel at an arbitrary location (x_0,y_0). As a result, a radially outspreading bending wave propagates from the source (x_0,y_0). The propagation of this bending wave in the upper panel is affected by the attached lattice core (rib-stiffeners), which transmits the motion to the bottom panel. Both panels are modeled as a classical thin plate, following Kirchhoff's thin plate theory. As the focus is placed on the intrinsic characteristics of bending wave propagation in the structure, air-structure coupling is ignored. The theoretical formulation presented below proposes a comprehensive analytic model for bending wave propagation in the sandwich structure, accounting for not only the tensional forces, bending and torsional moments of the orthogonal rib-stiffeners, but also their inertial effects.

2.2. Analytical formulation of panel vibration

Upon point force excitation, the vibration of the upper and bottom panels can be described using two dynamic governing equations, where the influence of the rib-stiffeners exists in the form of tensional forces (general force plus inertial force), bending moments (general bending moment plus inertial bending moment), and torsional moments (general torsional moment plus inertial torsional moment). With the inertial effects of the rib-stiffeners accounted for, the resultant tensional forces, bending and torsional moments acting on the upper and bottom panels per rib-stiffener are not equal, denoted here by (Q^+,M^+,M_T^+) and (Q^-,M^-,M_T^-),

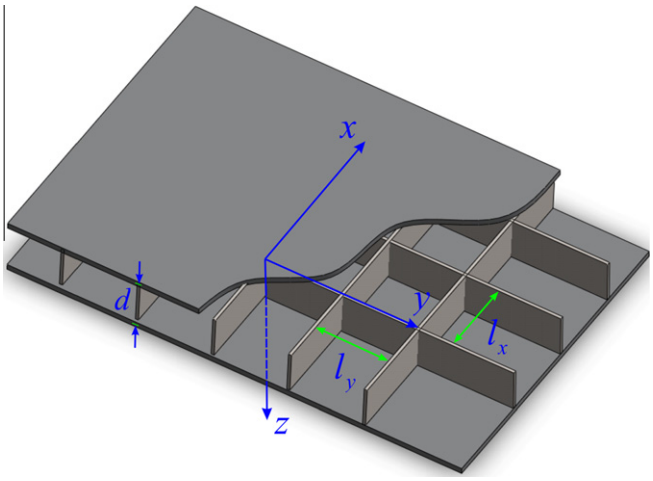

Fig. 1. Sandwich panel with orthogonally rib-stiffened core.

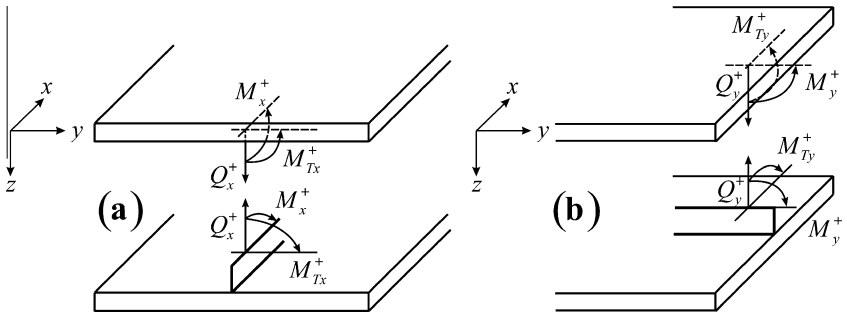

Fig. 2. Convention for tensional forces, bending moments and torsional moments between upper panel and (a) *x*-wise and (b) *y*-wise stiffeners.

respectively. Fig. 2 shows the convention employed for denoting the tensional forces as well as the bending and torsional moments between the upper panel and the *x*- and *y*-wise stiffeners. The same apply at the interface between the bottom panel and the *x*- and *y*-wise stiffeners.

Since the excitation is harmonic, the dynamic responses of the two panels should also be harmonic. For simplicity, the harmonic time term $e^{-i\omega t}$ is suppressed from the formulation below. The dynamic governing equations are thence given by:

$$\begin{aligned} D_1\nabla^4 w_1 + m_1\frac{\partial^2 w_1}{\partial t^2} &= \sum_m\left[Q_y^+\delta(x-ml_x) + \frac{\partial}{\partial y}\left\{M_y^+\delta(x-ml_x)\right\} + \frac{\partial}{\partial x}\left\{M_{Ty}^+\delta(x-ml_x)\right\}\right] \\ &+ \sum_n\left[Q_x^+\delta(y-nl_y) + \frac{\partial}{\partial x}\left\{M_x^+\delta(y-nl_y)\right\} + \frac{\partial}{\partial y}\left\{M_{Tx}^+\delta(y-nl_y)\right\}\right] \\ &+ q_0\delta(x-x_0)\delta(y-y_0) \end{aligned} \tag{1}$$

$$\begin{aligned} D_2\nabla^4 w_2 + m_2\frac{\partial^2 w_2}{\partial t^2} &= -\sum_m\left[Q_y^-\delta(x-ml_x) + \frac{\partial}{\partial y}\left\{M_y^-\delta(x-ml_x)\right\} + \frac{\partial}{\partial x}\left\{M_{Ty}^-\delta(x-ml_x)\right\}\right] \\ &- \sum_n\left[Q_x^-\delta(y-nl_y) + \frac{\partial}{\partial x}\left\{M_x^-\delta(y-nl_y)\right\} + \frac{\partial}{\partial y}\left\{M_{Tx}^-\delta(y-nl_y)\right\}\right] \end{aligned} \tag{2}$$

where $\nabla^4 \equiv (\partial^2/\partial x^2 + \partial^2/\partial y^2)^2$; $\delta(\cdot)$ is the Dirac delta function; (w_1, w_2), (m_1, m_2) and (D_1, D_2) are the displacement, surface mass density and flexural rigidity of the upper and bottom panel, respectively. The material loss factor η_j ($j = 1, 2$ for upper and bottom panel, respectively) is introduced with the complex Young's modulus as

$$D_j = \frac{E_j h_j^3(1+i\eta_j)}{12(1-\nu_j^2)} \quad (j=1,2) \tag{3}$$

As the factual forces and moments exerting on the upper and bottom panels are not the same due to the consideration of inertial forces and moments, the terms associated with the two panels are denoted separately by superscripts + (upper) and − (bottom). Subscripts *x* and *y* are introduced to represent those terms arising from the *x*- and *y*-wise stiffeners, respectively.

Taking into account the inertial effects (due to stiffener mass) and applying both the Hooke's law and Newton's second law, one obtains the tensional forces arising from the rib-stiffeners as [36]:

$$Q_x^+ = -\frac{K_x(K_x - m_x\omega^2)}{2K_x - m_x\omega^2}w_1 + \frac{K_x^2}{2K_x - m_x\omega^2}w_2 \tag{4}$$

$$Q_x^- = -\frac{K_x^2}{2K_x - m_x\omega^2}w_1 + \frac{K_x(K_x - m_x\omega^2)}{2K_x - m_x\omega^2}w_2 \tag{5}$$

$$Q_y^+ = -\frac{K_y(K_y - m_y\omega^2)}{2K_y - m_y\omega^2}w_1 + \frac{K_y^2}{2K_y - m_y\omega^2}w_2 \tag{6}$$

$$Q_y^- = -\frac{K_y^2}{2K_y - m_y\omega^2}w_1 + \frac{K_y(K_y - m_y\omega^2)}{2K_y - m_y\omega^2}w_2 \tag{7}$$

where ω is the circle frequency and (K_x, K_y) are the tensional stiffness of half the rib-stiffeners per unit length.

Similarly, the bending moments of the rib-stiffeners can be expressed as [36]:

$$M_x^+ = \frac{E_xI_x^*(E_xI_x^* - \rho_xI_x\omega^2)}{2E_xI_x^* - \rho_xI_x\omega^2}\frac{\partial^2 w_1}{\partial x^2} - \frac{E_x^2I_x^{*2}}{2E_xI_x^* - \rho_xI_x\omega^2}\frac{\partial^2 w_2}{\partial x^2} \tag{8}$$

$$M_x^- = \frac{E_x^2I_x^{*2}}{2E_xI_x^* - \rho_xI_x\omega^2}\frac{\partial^2 w_1}{\partial x^2} - \frac{E_xI_x^*(E_xI_x^* - \rho_xI_x\omega^2)}{2E_xI_x^* - \rho_xI_x\omega^2}\frac{\partial^2 w_2}{\partial x^2} \tag{9}$$

$$M_y^+ = \frac{E_yI_y^*(E_yI_y^* - \rho_yI_y\omega^2)}{2E_yI_y^* - \rho_yI_y\omega^2}\frac{\partial^2 w_1}{\partial y^2} - \frac{E_y^2I_y^{*2}}{2E_yI_y^* - \rho_yI_y\omega^2}\frac{\partial^2 w_2}{\partial y^2} \tag{10}$$

$$M_y^- = \frac{E_y^2I_y^{*2}}{2E_yI_y^* - \rho_yI_y\omega^2}\frac{\partial^2 w_1}{\partial y^2} - \frac{E_yI_y^*\left(E_yI_y^* - \rho_yI_y\omega^2\right)}{2E_yI_y^* - \rho_yI_y\omega^2}\frac{\partial^2 w_2}{\partial y^2} \tag{11}$$

where $\left(E_xI_x^*, E_yI_y^*\right)$ are the bending stiffness of half the rib-stiffeners, (ρ_x, ρ_y) and (I_x, I_y) are mass density and polar moment of inertia for the rib-stiffeners, with subscripts *x* and *y* indicating the direction of the stiffener.

Following similar procedures for deriving the tensional forces and bending moments, one obtains the torsional moments of the rib-stiffeners as [36]:

$$M_{Tx}^+ = \frac{G_xJ_x^*(G_xJ_x^* - \rho_xJ_x\omega^2)}{2G_xJ_x^* - \rho_xJ_x\omega^2}\frac{\partial^2 w_1}{\partial x\partial y} - \frac{G_x^2J_x^{*2}}{2G_xJ_x^* - \rho_xJ_x\omega^2}\frac{\partial^2 w_2}{\partial x\partial y} \tag{12}$$

$$M_{Tx}^- = \frac{G_x^2J_x^{*2}}{2G_xJ_x^* - \rho_xJ_x\omega^2}\frac{\partial^2 w_1}{\partial x\partial y} - \frac{G_xJ_x^*(G_xJ_x^* - \rho_xJ_x\omega^2)}{2G_xJ_x^* - \rho_xJ_x\omega^2}\frac{\partial^2 w_2}{\partial x\partial y} \tag{13}$$

$$M_{Ty}^+ = \frac{G_yJ_y^*\left(G_yJ_y^* - \rho_yJ_y\omega^2\right)}{2G_yJ_y^* - \rho_yJ_y\omega^2}\frac{\partial^2 w_1}{\partial y\partial x} - \frac{G_y^2J_y^{*2}}{2G_yJ_y^* - \rho_yJ_y\omega^2}\frac{\partial^2 w_2}{\partial y\partial x} \tag{14}$$

$$M_{Ty}^- = \frac{G_y^2J_y^{*2}}{2G_yJ_y^* - \rho_yJ_y\omega^2}\frac{\partial^2 w_1}{\partial y\partial x} - \frac{G_yJ_y^*\left(G_yJ_y^* - \rho_yJ_y\omega^2\right)}{2G_yJ_y^* - \rho_yJ_y\omega^2}\frac{\partial^2 w_2}{\partial y\partial x} \tag{15}$$

where $\left(G_xJ_x^*, G_yJ_y^*\right)$ are the torsional stiffness of half the rib-stiffeners and (J_x, J_y) are the torsional moment of inertia for the rib-stiffeners.

In the above expressions for the tensional forces, bending moments and torsional moments of a rib-stiffener, the geometrical properties of its cross-section are given by:

$$K_x = \frac{E_xt_x}{d/2}, \quad K_y = \frac{E_yt_y}{d/2} \tag{16}$$

$$I_x^* = \frac{t_x(d/2)^3}{12}, \quad I_y^* = \frac{t_y(d/2)^3}{12}, \quad I_x = \frac{t_xd^3}{12}, \quad I_y = \frac{t_yd^3}{12} \tag{17}$$

$$J_x^* = \frac{t_x^3 d}{2}\left[\frac{1}{3} - \frac{64}{\pi^5}\frac{2t_x}{d}\sum_{n=1,3,5,\ldots}^{\infty}\frac{\tanh(n\pi d/4t_x)}{n^5}\right] \tag{18}$$

$$J_y^* = \frac{t_y^3 d}{2}\left[\frac{1}{3} - \frac{64}{\pi^5}\frac{2t_y}{d}\sum_{n=1,3,5,\ldots}^{\infty}\frac{\tanh(n\pi d/4t_y)}{n^5}\right] \tag{19}$$

$$J_x = t_x^3 d\left[\frac{1}{3} - \frac{64}{\pi^5}\frac{t_x}{d}\sum_{n=1,3,5,\ldots}^{\infty}\frac{\tanh(n\pi d/2t_x)}{n^5}\right] \tag{20}$$

$$J_y = t_y^3 d\left[\frac{1}{3} - \frac{64}{\pi^5}\frac{t_y}{d}\sum_{n=1,3,5,\ldots}^{\infty}\frac{\tanh(n\pi d/2t_y)}{n^5}\right] \tag{21}$$

where E_x and E_y are separately the Young's modulus of the x- and y-wise stiffener materials.

To simplify Eqs. (4)–(15), the following set of specified characteristics is introduced to replace the coefficients of general displacements.

(1) Replacement of tensional force coefficients:

$$R_{Q1} = \frac{K_x(K_x - m_x\omega^2)}{2K_x - m_x\omega^2}, \quad R_{Q2} = \frac{K_x^2}{2K_x - m_x\omega^2} \tag{22}$$

$$R_{Q3} = \frac{K_y(K_y - m_y\omega^2)}{2K_y - m_y\omega^2}, \quad R_{Q4} = \frac{K_y^2}{2K_y - m_y\omega^2} \tag{23}$$

(2) Replacement of bending moment coefficients:

$$R_{M1} = \frac{E_x I_x^*(E_x I_x^* - \rho_x I_x\omega^2)}{2E_x I_x^* - \rho_x I_x\omega^2}, \quad R_{M2} = \frac{E_x^2 I_x^{*2}}{2E_x I_x^* - \rho_x I_x\omega^2} \tag{24}$$

$$R_{M3} = \frac{E_y I_y^*\left(E_y I_y^* - \rho_y I_y\omega^2\right)}{2E_y I_y^* - \rho_y I_y\omega^2}, \quad R_{M4} = \frac{E_y^2 I_y^{*2}}{2E_y I_y^* - \rho_y I_y\omega^2} \tag{25}$$

(3) Replacement of torsional moment coefficients:

$$R_{T1} = \frac{G_x J_x^*(G_x J_x^* - \rho_x J_x\omega^2)}{2G_x J_x^* - \rho_x J_x\omega^2}, \quad R_{T2} = \frac{G_x^2 J_x^{*2}}{2G_x J_x^* - \rho_x J_x\omega^2} \tag{26}$$

$$R_{T3} = \frac{G_y J_y^*\left(G_y J_y^* - \rho_y J_y\omega^2\right)}{2G_y J_y^* - \rho_y J_y\omega^2}, \quad R_{T4} = \frac{G_y^2 J_y^{*2}}{2G_y J_y^* - \rho_y J_y\omega^2} \tag{27}$$

Using Eqs. (22)–(27), one can simplify the expressions of the tensional forces, bending moments and torsional moments, as:

(1) Tensional forces:

$$Q_x^+ = -R_{Q1}w_1 + R_{Q2}w_2, \quad Q_x^- = -R_{Q2}w_1 + R_{Q1}w_2 \tag{28}$$

$$Q_y^+ = -R_{Q3}w_1 + R_{Q4}w_2, \quad Q_y^- = -R_{Q4}w_1 + R_{Q3}w_2 \tag{29}$$

(2) Bending moments:

$$M_x^+ = R_{M1}\frac{\partial^2 w_1}{\partial x^2} - R_{M2}\frac{\partial^2 w_2}{\partial x^2}, \quad M_x^- = R_{M2}\frac{\partial^2 w_1}{\partial x^2} - R_{M1}\frac{\partial^2 w_2}{\partial x^2} \tag{30}$$

$$M_y^+ = R_{M3}\frac{\partial^2 w_1}{\partial y^2} - R_{M4}\frac{\partial^2 w_2}{\partial y^2}, \quad M_y^- = R_{M4}\frac{\partial^2 w_1}{\partial y^2} - R_{M3}\frac{\partial^2 w_2}{\partial y^2} \tag{31}$$

(3) Torsional moments:

$$M_{Tx}^+ = R_{T1}\frac{\partial^2 w_1}{\partial x\partial y} - R_{T2}\frac{\partial^2 w_2}{\partial x\partial y}, \quad M_{Tx}^- = R_{T2}\frac{\partial^2 w_1}{\partial x\partial y} - R_{T1}\frac{\partial^2 w_2}{\partial x\partial y} \tag{32}$$

$$M_{Ty}^+ = R_{T3}\frac{\partial^2 w_1}{\partial y\partial x} - R_{T4}\frac{\partial^2 w_2}{\partial y\partial x}, \quad M_{Ty}^- = R_{T4}\frac{\partial^2 w_1}{\partial y\partial x} - R_{T3}\frac{\partial^2 w_2}{\partial y\partial x} \tag{33}$$

2.3. Solutions

Fully considering the periodic nature of the present sandwich structure and applying the Poisson summation formula [5,25], one can write the wave components in the periodic structure using space harmonic series, as:

$$\sum_m \delta(x - ml_x) = \frac{1}{l_x}\sum_m e^{-i(2m\pi/l_x)x} \tag{34}$$

$$\sum_n \delta(y - nl_y) = \frac{1}{l_y}\sum_n e^{-i(2n\pi/l_y)y} \tag{35}$$

The displacement of each panel is a function of coordinates (x,y) as well as the Fourier transform of its wavenumber frequency, the latter being also a function of the wavenumbers (k_x,k_y). The Fourier transform pair relating these two quantities with respect to (x,y) and (k_x,k_y) can be written as:

$$w(x,y) = \int_{-\infty}^{+\infty}\int_{-\infty}^{+\infty}\tilde{w}(k_x,k_y)e^{i(k_x x + k_y y)}dk_x\,dk_y \tag{36}$$

$$\tilde{w}(k_x,k_y) = \left(\frac{1}{2\pi}\right)^2\int_{-\infty}^{+\infty}\int_{-\infty}^{+\infty}w(x,y)e^{-i(k_x x + k_y y)}dx\,dy \tag{37}$$

Employing Eqs. (34) and (35) and then taking the Fourier transform and replacing the wavenumbers (k_x,k_y) by (α,β), respectively, one can rewrite the governing Eqs. (1) and (2) as:

$$\begin{aligned}\tilde{w}_1(\alpha,\beta) = {} & \frac{1}{D_1 l_x f_1(\alpha,\beta)}\sum_m\left[\tilde{Q}_y^+(\alpha_m,\beta) + i\beta\tilde{M}_y^+(\alpha_m,\beta) + i\alpha\tilde{M}_{Ty}^+(\alpha_m,\beta)\right] \\ & + \frac{1}{D_1 l_y f_1(\alpha,\beta)}\sum_n\left[\tilde{Q}_x^+(\alpha,\beta_n) + i\alpha\tilde{M}_x^+(\alpha,\beta_n) + i\beta\tilde{M}_{Tx}^+(\alpha,\beta_n)\right] \\ & + \frac{q_0 e^{-i(\alpha x_0 + \beta y_0)}}{(2\pi)^2 D_1 f_1(\alpha,\beta)}\end{aligned} \tag{38}$$

$$\begin{aligned}\tilde{w}_2(\alpha,\beta) = {} & \frac{-1}{D_2 l_x f_2(\alpha,\beta)}\sum_m\left[\tilde{Q}_y^-(\alpha_m,\beta) + i\beta\tilde{M}_y^-(\alpha_m,\beta) + i\alpha\tilde{M}_{Ty}^-(\alpha_m,\beta)\right] \\ & - \frac{1}{D_2 l_y f_2(\alpha,\beta)}\sum_n\left[\tilde{Q}_x^-(\alpha,\beta_n) + i\alpha\tilde{M}_x^-(\alpha,\beta_n) + i\beta\tilde{M}_{Tx}^-(\alpha,\beta_n)\right]\end{aligned} \tag{39}$$

where the dependence of a term on wavenumbers (α,β) is indicated using the hat sign $\sim$, meaning the corresponding Fourier transform of this term. For instance, $(\tilde{w}_1,\tilde{w}_2)$ are the Fourier transforms of (w_1,w_2). The Fourier transforms of the tensional forces, bending moments and torsional moments are presented below.

(1) Fourier transforms of tensional forces:

$$\tilde{Q}_x^+(a,\beta_n) = -R_{Q1}\tilde{w}_1(a,\beta_n) + R_{Q2}\tilde{w}_2(a,\beta_n) \tag{40}$$

$$\tilde{Q}_x^-(a,\beta_n) = -R_{Q2}\tilde{w}_1(a,\beta_n) + R_{Q1}\tilde{w}_2(a,\beta_n) \tag{41}$$

$$\tilde{Q}_y^+(a_m,\beta) = -R_{Q3}\tilde{w}_1(a_m,\beta) + R_{Q4}\tilde{w}_2(a_m,\beta) \tag{42}$$

$$\tilde{Q}_y^-(a_m,\beta) = -R_{Q4}\tilde{w}_1(a_m,\beta) + R_{Q3}\tilde{w}_2(a_m,\beta) \tag{43}$$

(2) Fourier transforms of bending moments:

$$\tilde{M}_x^+(a,\beta_n) = -\alpha^2[R_{M1}\tilde{w}_1(a,\beta_n) - R_{M2}\tilde{w}_2(a,\beta_n)] \tag{44}$$

$$\tilde{M}_x^-(a,\beta_n) = -\alpha^2[R_{M2}\tilde{w}_1(a,\beta_n) - R_{M1}\tilde{w}_2(a,\beta_n)] \tag{45}$$

$$\tilde{M}_y^+(a_m,\beta) = -\beta^2[R_{M3}\tilde{w}_1(a_m,\beta) - R_{M4}\tilde{w}_2(a_m,\beta)] \tag{46}$$

$$\tilde{M}_y^-(a_m,\beta) = -\beta^2[R_{M4}\tilde{w}_1(a_m,\beta) - R_{M3}\tilde{w}_2(a_m,\beta)] \tag{47}$$

(3) Fourier transforms of torsional moments:

$$\tilde{M}^{+}_{Tx}(a,\beta_n) = -\alpha\beta_n[R_{T1}\tilde{w}_1(a,\beta_n) - R_{T2}\tilde{w}_2(a,\beta_n)] \quad (48)$$

$$\tilde{M}^{-}_{Tx}(a,\beta_n) = -\alpha\beta_n[R_{T2}\tilde{w}_1(a,\beta_n) - R_{T1}\tilde{w}_2(a,\beta_n)] \quad (49)$$

$$\tilde{M}^{+}_{Ty}(a_m,\beta) = -\alpha_m\beta[R_{T3}\tilde{w}_1(a_m,\beta) - R_{T4}\tilde{w}_2(a_m,\beta)] \quad (50)$$

$$\tilde{M}^{-}_{Ty}(a_m,\beta) = -\alpha_m\beta[R_{T4}\tilde{w}_1(a_m,\beta) - R_{T3}\tilde{w}_2(a_m,\beta)] \quad (51)$$

Substitution of (40)–(51) into (38) and (39) yields:

$$\begin{aligned}\tilde{w}_1(\alpha,\beta) = {} & \frac{1}{D_1 l_x f_1(\alpha,\beta)}\sum_m\left[-R_{Q3} - i\beta^3 R_{M3} - i\alpha\alpha_m\beta R_{T3}\right]\tilde{w}_1(\alpha_m,\beta)\\ & + \frac{1}{D_1 l_y f_1(\alpha,\beta)}\sum_n\left[-R_{Q1} - i\alpha^3 R_{M1} - i\alpha\beta\beta_n R_{T1}\right]\tilde{w}_1(\alpha,\beta_n)\\ & + \frac{1}{D_1 l_x f_1(\alpha,\beta)}\sum_m\left[R_{Q4} + i\beta^3 R_{M4} + i\alpha\alpha_m\beta R_{T4}\right]\tilde{w}_2(\alpha_m,\beta)\\ & + \frac{1}{D_1 l_y f_1(\alpha,\beta)}\sum_n\left[R_{Q2} + i\alpha^3 R_{M2} + i\alpha\beta\beta_n R_{T2}\right]\tilde{w}_2(\alpha,\beta_n)\\ & + \frac{q_0 e^{-i(\alpha x_0+\beta y_0)}}{(2\pi)^2 D_1 f_1(\alpha,\beta)}\end{aligned} \quad (52)$$

$$\begin{aligned}\tilde{w}_2(\alpha,\beta) = {} & \frac{-1}{D_2 l_x f_2(\alpha,\beta)}\sum_m\left[-R_{Q4} - i\beta^3 R_{M4} - i\alpha\alpha_m\beta R_{T4}\right]\tilde{w}_1(\alpha_m,\beta)\\ & - \frac{1}{D_2 l_y f_2(\alpha,\beta)}\sum_n\left[-R_{Q2} - i\alpha^3 R_{M2} - i\alpha\beta\beta_n R_{T2}\right]\tilde{w}_1(\alpha,\beta_n)\\ & - \frac{1}{D_2 l_x f_2(\alpha,\beta)}\sum_m\left[R_{Q3} + i\beta^3 R_{M3} + i\alpha\alpha_m\beta R_{T3}\right]\tilde{w}_2(\alpha_m,\beta)\\ & - \frac{1}{D_2 l_y f_2(\alpha,\beta)}\sum_n\left[R_{Q1} + i\alpha^3 R_{M1} + i\alpha\beta\beta_n R_{T1}\right]\tilde{w}_2(\alpha,\beta_n)\end{aligned} \quad (53)$$

where

$$f_1(\alpha,\beta) = (\alpha^2+\beta^2)^2 - m_1\omega^2/D_1, \quad f_2(\alpha,\beta) = (\alpha^2+\beta^2)^2 - m_2\omega^2/D_2 \quad (54)$$

$$\alpha_m = \alpha + 2m\pi/l_x, \quad \beta_n = \beta + 2n\pi/l_y \quad (55)$$

To solve Eqs. (52) and (53), one needs to replace (α,β) by (α'_m,β'_n), resulting in two sets of simultaneous algebraic equations:

$$\begin{aligned}&\tilde{w}_1(\alpha'_m,\beta'_n) + \frac{R_{Q3}+i\beta'^3_n R_{M3}}{D_1 l_x f_1(\alpha'_m,\beta'_n)}\sum_m\tilde{w}_1(\alpha_m,\beta'_n)\\ &+ \frac{i\alpha'_m\beta'_n R_{T3}}{D_1 l_x f_1(\alpha'_m,\beta'_n)}\sum_m\alpha_m\tilde{w}_1(\alpha_m,\beta'_n) + \frac{R_{Q1}+i\alpha'^3_m R_{M1}}{D_1 l_y f_1(\alpha'_m,\beta'_n)}\sum_n\tilde{w}_1(\alpha'_m,\beta_n)\\ &+ \frac{i\alpha'_m\beta'_n R_{T1}}{D_1 l_y f_1(\alpha'_m,\beta'_n)}\sum_n\beta_n\tilde{w}_1(\alpha'_m,\beta_n) - \frac{R_{Q4}+i\beta'^3_n R_{M4}}{D_1 l_x f_1(\alpha'_m,\beta'_n)}\sum_m\tilde{w}_2(\alpha_m,\beta'_n)\\ &- \frac{i\alpha'_m\beta'_n R_{T4}}{D_1 l_x f_1(\alpha'_m,\beta'_n)}\sum_m\alpha_m\tilde{w}_2(\alpha_m,\beta'_n) - \frac{R_{Q2}+i\alpha'^3_m R_{M2}}{D_1 l_y f_1(\alpha'_m,\beta'_n)}\sum_n\tilde{w}_2(\alpha'_m,\beta_n)\\ &- \frac{i\alpha'_m\beta'_n R_{T2}}{D_1 l_y f_1(\alpha'_m,\beta'_n)}\sum_n\beta_n\tilde{w}_2(\alpha'_m,\beta_n) = \frac{q_0 e^{-i(\alpha'_m x_0+\beta'_n y_0)}}{(2\pi)^2 D_1 f_1(\alpha'_m,\beta'_n)}\end{aligned} \quad (56)$$

$$\begin{aligned}&-\frac{R_{Q4}+i\beta'^3_n R_{M4}}{D_2 l_x f_2(\alpha'_m,\beta'_n)}\sum_m\tilde{w}_1(\alpha_m,\beta'_n) - \frac{i\alpha'_m\beta'_n R_{T4}}{D_2 l_x f_2(\alpha'_m,\beta'_n)}\sum_m\alpha_m\tilde{w}_1(\alpha_m,\beta'_n)\\ &- \frac{R_{Q2}+i\alpha'^3_m R_{M2}}{D_2 l_y f_2(\alpha'_m,\beta'_n)}\sum_n\tilde{w}_1(\alpha'_m,\beta_n) - \frac{i\alpha'_m\beta'_n R_{T2}}{D_2 l_y f_2(\alpha'_m,\beta'_n)}\sum_n\beta_n\tilde{w}_1(\alpha'_m,\beta_n)\\ &+ \tilde{w}_2(\alpha'_m,\beta'_n) + \frac{R_{Q3}+i\beta'^3_n R_{M3}}{D_2 l_x f_2(\alpha'_m,\beta'_n)}\sum_m\tilde{w}_2(\alpha_m,\beta'_n)\\ &+ \frac{i\alpha'_m\beta'_n R_{T3}}{D_2 l_x f_2(\alpha'_m,\beta'_n)}\sum_m\alpha_m\tilde{w}_2(\alpha_m,\beta'_n) + \frac{R_{Q1}+i\alpha'^3_m R_{M1}}{D_2 l_y f_2(\alpha'_m,\beta'_n)}\sum_n\tilde{w}_2(\alpha'_m,\beta_n)\\ &+ \frac{i\alpha'_m\beta'_n R_{T1}}{D_2 l_y f_2(\alpha'_m,\beta'_n)}\sum_n\beta_n\tilde{w}_2(\alpha'_m,\beta_n) = 0\end{aligned} \quad (57)$$

which contain two sets of infinite unknowns: $\tilde{w}_1(\alpha'_m,\beta'_n)$ and $\tilde{w}_2(\alpha'_m,\beta'_n)$, with $m = -\infty$ to $+\infty$ and $n = -\infty$ to $+\infty$. Insofar as the solution converges, these equations can be solved simultaneously by truncation. That is, (m,n) only take values in a finite range of $m = -\hat{m}$ to $\hat{m}$ and $n = -\hat{n}$ to $\hat{n}$ (where $\hat{m}$ and $\hat{n}$ both being positive integer). For brevity, the resulting simultaneous equations containing a finite number [i.e., $2MN$, where $M = 2\hat{m}+1$, $N = 2\hat{n}+1$] of unknowns can be expressed in matrix form, as:

$$\begin{bmatrix} T_{11} & T_{12} \\ T_{21} & T_{22} \end{bmatrix}_{2MN\times 2MN}\begin{Bmatrix} \tilde{w}_1(\alpha'_m,\beta'_n) \\ \tilde{w}_2(\alpha'_m,\beta'_n) \end{Bmatrix}_{2MN\times 1} = \begin{Bmatrix} F_{mn} \\ 0 \end{Bmatrix}_{2MN\times 1} \quad (58)$$

Eq. (57) can be solved numerically to obtain the panel displacements $\tilde{w}_1(\alpha,\beta)$ and $\tilde{w}_2(\alpha,\beta)$ in their respective wavenumber space. Details of the derivation are presented in Appendix A.

3. Far field radiated sound pressure

The radiated sound pressure is related directly to the dynamic response of the radiating panel (bottom panel in the present case). Once the dynamic response of the bottom panel $\tilde{w}_2(\alpha,\beta)$ is solved, the radiated sound pressure at far field can be obtained.

Due to the periodic nature of the sandwich, upon excitation by a harmonic point force on its upper panel, a series of space harmonic waves are transmitting in the structure. For a given point force with wavenumbers (α_0,β_0), a flexural wave having the same wavenumbers (α_0,β_0) is excited and propagates in the face panel. It will generate the (m,n)th harmonic wavenumber components $(a_0 + 2m\pi/l_x, \beta_0 + 2n\pi/l_y)$ owing to the vibration interaction of the face panel with the mth x-wise and nth y-wise stiffeners. Therefore, the face panel vibration and the radiated sound pressure both contain a series of space harmonic wave components with wavenumbers $(a_0 + 2m\pi/l_x, \beta_0 + 2n\pi/l_y)$, where $-\infty < m < +\infty$ and $-\infty < n < +\infty$.

With the origin of the spherical coordinates (r,θ,φ) located at the excitation point (x_0,y_0), the far field sound pressure $p(r,\theta,\varphi)$ radiated from a vibrating surface with displacement $w(x,y)$ is given by [37]:

$$p(r,\theta,\varphi) = -\frac{\rho_0\omega^2 e^{ik_0 r}}{2\pi r}e^{i(\alpha x_0+\beta y_0)}\int_{-\infty}^{+\infty}\int_{-\infty}^{+\infty} w(x,y)e^{-i(\alpha x+\beta y)}dx\,dy \quad (59)$$

where $k_0 = \omega/c_0$, c_0 and ρ_0 being the sound speed and air density, respectively, and the wavenumbers α and β are:

$$\alpha = k_0\cos\varphi\sin\theta, \quad \beta = k_0\sin\varphi\sin\theta \quad (60)$$

Finally, with the Fourier transform of (37), Eq. (59) becomes:

$$p(r,\theta,\varphi) = -2\pi\rho_0\omega^2(e^{ik_0 r}/r)e^{i(\alpha x_0+\beta y_0)}\tilde{w}(\alpha,\beta) \quad (61)$$

4. Numerical results and discussion

With the modeling presented above describing accurately the dynamic response of an infinite orthogonally rib-stiffened sandwich structure excited by a point force and the formulation for the far field radiated sound pressure, the on-axis (i.e., on the axis $\theta = \varphi = 0$) far field pressure is calculated below to explore the sound radiation characteristics of the structure. Note that on the selected axis (i.e., $\theta = \varphi = 0$), the stationary phase wavenumbers $\bar{\alpha}$ and $\bar{\beta}$ are both zero.

The simultaneous algebraic equations are truncated at the $\pm\hat{m}$ and $\pm\hat{n}$ harmonic wave components in the x- and y-directions, with the frequency dependent $\hat{m}$ and $\hat{n}$ selected as 3 and 10 at 100 Hz and 10 kHz, respectively. Numerical convergence tests have ensured that these $\hat{m}$ and $\hat{n}$ values are sufficient large for obtaining

accurate results. For numerical analysis, the material properties and structural dimensions of the sandwich are taken as follows. The panels (facesheets) and rib-stiffeners are made of aluminum, with Young's modulus $E = 70$ GPa, density $\rho = 2700$ kg/m^3, Poisson ratio $\nu = 0.33$, and loss factor $\eta_1 = \eta_2 = 0.01$. The two facesheets have identical thickness $h = 0.002$ m (see Fig. 1). For simplicity, it is assumed that the ribs have square cross-sections, so that $t_x = t_y$. The depth of the air cavity (i.e., height of rib connections) is $d = 0.025$ m. The density of air is $\rho_0 = 1.21$ kg/m^3, sound speed in air is $c_0 = 343$ m/s, and the amplitude of the point force excitation is 1 N.

For reference, the high frequency asymptote of the far field sound pressure radiated by an unstiffened plate [5] is:

$$p_a = \frac{\rho_0 q_0}{2\pi m}\frac{e^{ik_0 r}}{r} \tag{62}$$

The far field sound pressure radiated by the present orthogonally rib-stiffened sandwich structure is then given in the form of sound pressure level (SPL) in decibel scales (dB) relative to p_a as:

$$SPL = 20 \cdot \log_{10}\left(\frac{p}{p_a}\right) \tag{63}$$

4.1. Validation of theoretical modeling

To verify the accuracy and applicability of the present theoretical modeling on wave propagation and sound radiation behavior of an orthogonally rib-stiffened sandwich structure, results obtained using the model are compared with those of Mace [5] for sound radiation from an orthogonally rib-stiffened single plate. To facilitate the comparison, the key parameters (i.e., Yong's modulus E, density ρ and thickness h) of the bottom panel are set to negligibly small in comparison with those of the upper panel and rib-stiffeners, so that the orthogonally rib-stiffened sandwich behaves exactly like an orthogonally rib-stiffened single plate.

For the purpose of validation, the material and geometric properties (Table 1) used by Mace [5] are adopted in the numerical calculations. Figs. 3 and 4 present the results for two different excitation locations, $(l_x/3, l_y/3)$ and $(l_x/2, l_y/2)$. Overall, good agreement is achieved between the present results and Mace's model prediction for both excitation locations. The discrepancies at high frequencies between the two different models, however, are attributed to the fact that the inertial effects and torsional moments of the rib-stiffeners were not account for by Mace [5]. The reason that at high frequency range the deviation is small in Fig. 3 but significant in Fig. 4 is because the excitation exerted at $(l_x/2, l_y/2)$ leads to stronger torsional moments of the rib-stiffeners than that exerted at $(l_x/3, l_y/3)$.

4.2. Influences of inertial effects arising from rib-stiffener mass

The inertial effects of the tensional forces, bending moments and torsional moments arising from the rib-stiffeners have been accounted for by the present analytical model. The influence of the inertial effects is explored below by comparing the predictions obtained for orthogonally rib-stiffened sandwich structures with and without considering the inertial effects.

Table 1
Material and geometric properties of orthogonally rib-stiffened single plate [5].

Plate			Fluid media	
D	m	η	ρ_0	c_0
2326 N m	39.1 kg/m	0.02	1000 kg/m^3	1500 m/s
Rib-stiffeners				
E	ρ	$l_x = l_y$	$t_x = t_y$	d
195 GPa	7700 kg/m^3	0.2 m	0.00508 m	0.0508 m

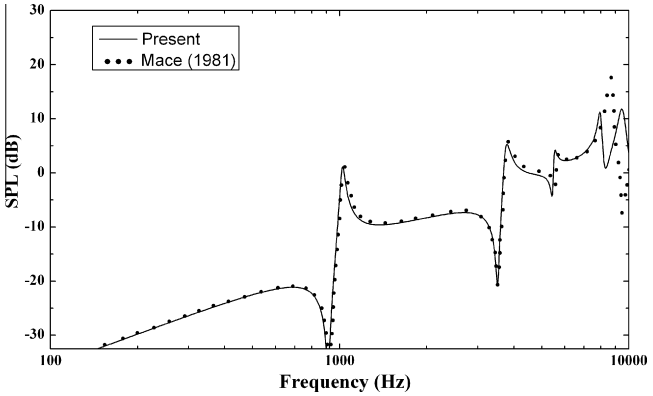

Fig. 3. Comparison between present model predictions and Mace's results for sound pressure level radiated by orthogonally rib-stiffened single plate excited at $(l_x/3, l_y/3)$.

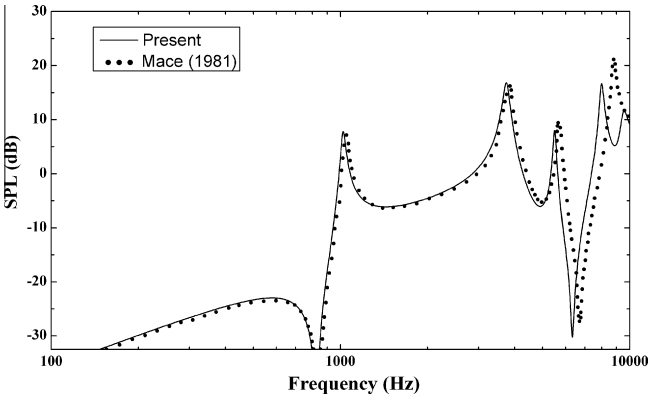

Fig. 4. Comparison between present model predictions and Mace's results for sound pressure level radiated by orthogonally rib-stiffened single plate excited at $(l_x/2, l_y/2)$.

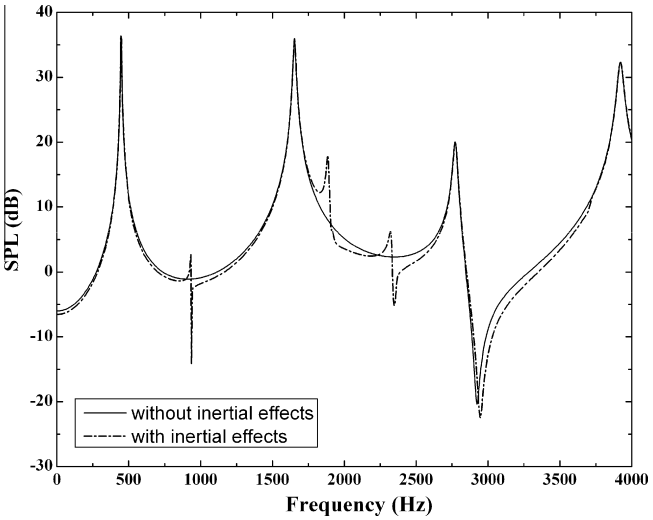

Fig. 5. Variation of on-axis far field radiated sound pressure with excitation frequency: influence of inertial effects. Geometry of rib-stiffeners: $t_x = t_y = 1$ mm, $l_x = l_y = 0.2$ m; excitation location: $(x_0, y_0) = (l_x/2, l_y/2)$.

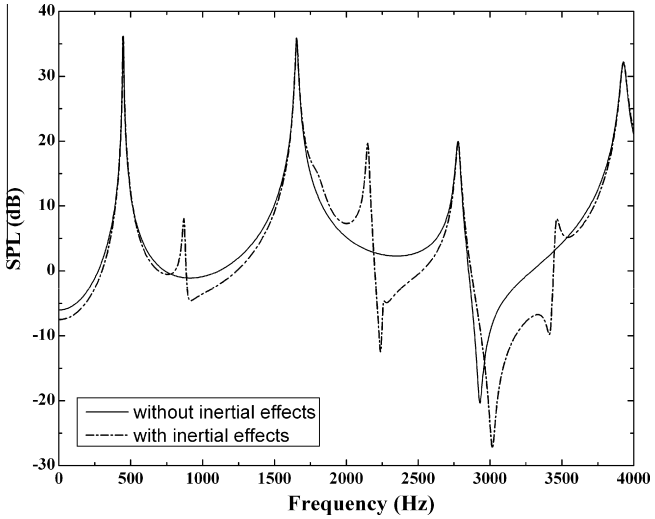

Fig. 6. Variation of on-axis far field radiated sound pressure with excitation frequency: influence of inertial effects. Geometry of rib-stiffeners: $t_x = t_y = 3$ mm, $l_x = l_y = 0.2$ m; excitation location: $(x_0, y_0) = (l_x/2, l_y/2)$.

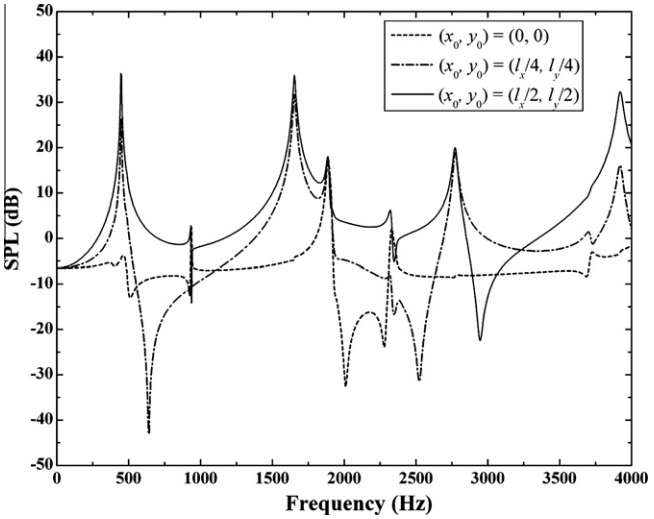

Fig. 7. On-axis far field radiated sound pressure plotted as a function of excitation frequency for selected excitation positions: $(x_0/l_x, y_0/l_y)$ at (0,0), (1/4,1/4), (1/2,1/2). Geometry of rib-stiffeners: $t_x = t_y = 1$ mm, $l_x = l_y = 0.2$ m.

With the point force acting at $(l_x/2, l_y/2)$, Figs. 5 and 6 plot the on-axis far field radiated sound pressure level as a function of excitation frequency for rib-stiffeners having square cross-sections, with width $t_x = t_y = 1$ mm and $t_x = t_y = 3$ mm, respectively. It can be seen from Fig. 5 that the SPL curve with the inertial effects considered has a tendency similar to that without considering inertial effects, the main discrepancy being the existence of several additional peaks and dips in the former. The superposition peaks (or dips) between the inertial case and the non-inertial one are dominated by face panel vibration, which are closely related to the maximum (or minimal) sound radiation wave shapes and vibration patterns. The appearance of the additional peaks and dips controlled predominantly by the rib-stiffeners is, on the other hand, attributed to the inertial effects arising from the mass of the rib-stiffeners. By comparing Fig. 5 with Fig. 6, it is seen that the discrepancy between the inertial and non-initial cases is enlarged when the thickness (or, equivalently, the mass) of the rib-stiffeners is increased.

4.3. Influence of excitation position

Whilst the amplitude of any point in wave mode shape depends strongly on its position, the radiating modes excited by a point force vary with the excitation position. It is therefore expected that the on-axis far field radiated sound pressure is significantly affected by the excitation position, which is confirmed by plotting in Fig. 7 the sound pressure level as a function of excitation frequency for three different excitation positions, i.e., $(x_0/l_x, y_0/l_y)$ at (0,0), (1/4,1/4), (1/2,1/2).

It is seen from Fig. 7 that the SPL curves of the (1/4,1/4) and (1/2,1/2) cases have peaks appearing at the same frequencies (e.g., 445, 1659, 2769 and 3919 Hz), although there exists large discrepancies at other frequencies (e.g., 3919 Hz in particular). In comparison, there are no evident peaks appearing in the SPL curve of the (0,0) case at these frequencies. As these radiated sound pressure peaks are mainly controlled by the wave mode shapes and vibration patterns of the face panel, it appears that the point force excitation at (1/4,1/4) and (1/2,1/2) can excite the appropriate radiating mode of the face panel. In contrast, the excitation at (0,0) is located at the joint connecting the face panel with the x- and y-wise rib-stiffeners, which excites mainly the tensional and bending motions of the x- and y-wise rib-stiffeners. Therefore, no SPL peaks appear for the (0,0) case at radiating frequencies controlled by panel vibration.

The radiating sound pressure peaks dominated by the rib-stiffeners are well captured by the three SPL curves of Fig. 7 at the same frequencies (e.g., 936, 1888, 2329, 3722 Hz), although some peaks may not be so evident due to complicated wave interaction at the junctions of panel, x-wise and y-wise stiffeners.

4.4. Influence of rib-stiffener spacings

As the periodicity spacings l_x and l_y between rib-stiffeners are key parameters describing the periodic nature of the sandwich structure (Fig. 1), they should influence significantly the wave propagation and sound radiation characteristics of the structure. Fig. 8 illustrates the influence of the periodicity spacings on radiated sound pressure by plotting the SPL curve tendencies, with (l_x, l_y) selected as (0.2,0.2) m, (0.225,0.225) m and (0.25,0.25) m, respectively, and the point force excitation fixed at $(l_x/2, l_y/2)$.

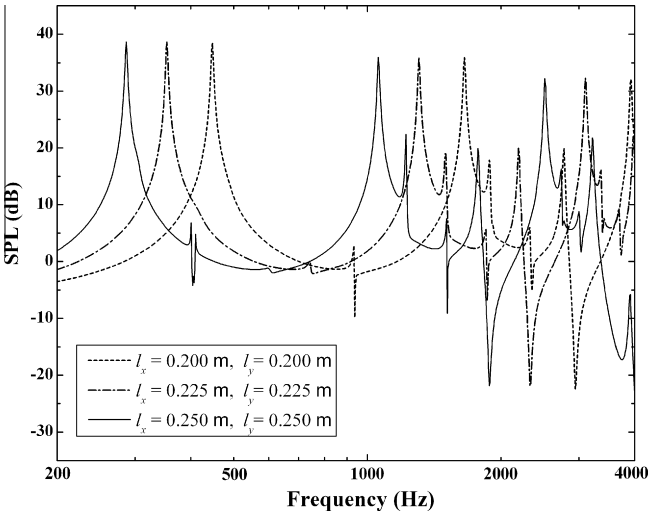

Fig. 8. Variation of on-axis far field radiated sound pressure with excitation frequency: influence of periodicity spacings between rib-stiffeners. Geometry of rib-stiffeners: $t_x = t_y = 1$ mm; excitation position: $(x_0, y_0) = (l_x/2, l_y/2)$.

The most attractive point about the results of Fig. 8 is that the magnitudes of the SPL peaks and dips (not only the panel vibration dominated but also the rib-stiffeners vibration controlled) decrease as the periodicity spacings are increased. However, overall, the three SPL curves exhibit almost the same tendency although their peaks and dips shift, which is attributed to the highly similar periodic nature of the sandwich structures.

There exists another interesting problem that what are the possible effects of breaking the assumed perfect periodicity of the structure. As well known, in perfectly periodic rib-stiffened structures, waves can propagate throughout all the structures; while disorder can lead to the appearance of localization phenomena of waves in mistuned periodic structures [38,39]. The existence of wave localization in disordered periodic structures induces a spatial decay of wave amplitude, as a result, the vibration and sound radiation of the structures will be reduced significantly. To squarely address this issue, the localization factor that characterizes the average exponential rates of decay of wave amplitudes should be applied to explore the detailed effects of disordered periodicity of the structures. Actually, this point should be our future work.

5. Conclusions

An analytic model has been formulated to investigate the wave propagation and sound radiation behavior of a point force-excited sandwich structure having two sets of orthogonal rib-stiffeners as its core. Unlike previous researches on rib-stiffened panel without considering the inertial effects of rib-stiffeners, the vibration motion of the rib-stiffeners is accurately described by introducing their tensional forces, bending moments and torsional moments as well as the corresponding inertial terms into the governing equations of the two face panels. The Fourier transform technique and Poisson summation formula are employed to solve the governing equations. The resulting two sets of infinite simultaneous algebraic equations are numerically solved by truncation insofar as the solution converges.

The far field sound radiation is examined to gain physical insights of the vibroacoustic response of the sandwich structure. First, comparisons between model predictions with previous published results for orthogonally stiffened single plates validate the accuracy and feasibility of the present analytic model, which also confirm the necessity of accounting for the inertial effects and torsional moments of the rib-stiffeners in any theoretical modeling. Subsequently, the influences of the excitation position, periodicity spacings of rib-stiffeners, and inertial effects rooted in the rib-stiffener mass upon the far field sound pressure radiated from the orthogonal sandwich structure are explored.

Since the inertial effects of the rib-stiffeners are considered in the present analytical model, a couple of additional peaks and dips on the SPL versus excitation frequency curve related to the inertial effects are well captured, which are especially evident when the mass of the rib-stiffeners is significant. Besides these rib-stiffener controlled SPL peaks and dips, it is also found that there exist panel controlled peaks and dips, which are related to certain wave shapes and vibration patterns possessing maximal or minimal sound radiation.

The excitation position of the point force plays a significant role in the wave propagation and sound radiation behavior of the sandwich, as different positions can excite different wave mode shape and vibration patterns of the face panel, resulting in either panel or rib-stiffener controlled vibration. Therefore, different peaks and dips associated with the panel or rib-stiffener controlled vibration will emerge and noticeably affect the tendency of the SPL curve.

As a key parameter describing the periodic nature of the sandwich structure, rib-stiffener spacing also has a dominant role. All the SPL peaks and dips dominantly controlled by either panel vibration or rib-stiffener vibration are shifted to lower frequencies as the periodicity spacings are increased. The overall tendency of the SPL curves remains nonetheless unchanged, owing to the similar periodic nature of the sandwich structures.

Acknowledgements

This work is supported by the National Basic Research Program of China (2011CB6103005), the National 111 Project of China (B06024), the National Natural Science Foundation of China (11072188 and 10825210) and the Shaanxi Province 13115 project (S2010ZDKG704).

Appendix A. Derivation of Eq. (58)

The displacement components of the two face panels in wavenumber space are:

$$\{\tilde{w}_1(\alpha'_m,\beta'_n)\} = [\,\tilde{w}_1(\alpha'_1,\beta'_1)\quad \tilde{w}_1(\alpha'_2,\beta'_1)\quad\cdots\quad \tilde{w}_1(\alpha'_M,\beta'_1)\quad \tilde{w}_1(\alpha'_1,\beta'_2)\quad \tilde{w}_1(\alpha'_2,\beta'_2)\quad\cdots\quad \tilde{w}_1(\alpha'_M,\beta'_2)\quad\cdots\quad \tilde{w}_1(\alpha'_M,\beta'_N)\,]^T_{MN\times 1} \tag{A.1}$$

$$\{\tilde{w}_2(\alpha'_m,\beta'_n)\} = [\,\tilde{w}_2(\alpha'_1,\beta'_1)\quad \tilde{w}_2(\alpha'_2,\beta'_1)\quad\cdots\quad \tilde{w}_2(\alpha'_M,\beta'_1)\quad \tilde{w}_2(\alpha'_1,\beta'_2)\quad \tilde{w}_2(\alpha'_2,\beta'_2)\quad\cdots\quad \tilde{w}_2(\alpha'_M,\beta'_2)\quad\cdots\quad \tilde{w}_2(\alpha'_M,\beta'_N)\,]^T_{MN\times 1} \tag{A.2}$$

The left-hand side of Eq. (58) represents the generalized force:

$$\{F_{mn}\} = [\,F_{11}\quad F_{21}\quad\cdots\quad F_{M1}\quad F_{12}\quad F_{22}\quad\cdots\quad F_{M2}\quad\cdots\quad F_{MN}\,]^T_{MN\times 1} \tag{A.3}$$

where

$$F_{mn} = \frac{q_0 e^{-i\left(\alpha'_m x_0+\beta'_n y_0\right)}}{(2\pi)^2 D_1 f_1(\alpha'_m,\beta'_n)} \tag{A.4}$$

$$T_{11,1} = \begin{bmatrix} 1 & & & \\ & 1 & & \\ & & \ddots & \\ & & & 1 \end{bmatrix}_{MN\times MN} \tag{A.5}$$

$$T_{22,1} = \begin{bmatrix} 1 & & & \\ & 1 & & \\ & & \ddots & \\ & & & 1 \end{bmatrix}_{MN\times MN} \tag{A.6}$$

$$\lambda^{11,2}_{Mn,j}=\begin{bmatrix}\frac{R_{Q3}+i\beta_n'^3R_{M3}}{D_jl_xf_j(\alpha_1',\beta_n')} & \frac{R_{Q3}+i\beta_n'^3R_{M3}}{D_jl_xf_j(\alpha_1',\beta_n')} & \cdots & \frac{R_{Q3}+i\beta_n'^3R_{M3}}{D_jl_xf_j(\alpha_1',\beta_n')}\\ \frac{R_{Q3}+i\beta_n'^3R_{M3}}{D_jl_xf_j(\alpha_2',\beta_n')} & \frac{R_{Q3}+i\beta_n'^3R_{M3}}{D_jl_xf_j(\alpha_2',\beta_n')} & \cdots & \frac{R_{Q3}+i\beta_n'^3R_{M3}}{D_jl_xf_j(\alpha_2',\beta_n')}\\ \vdots & \vdots & \ddots & \vdots\\ \frac{R_{Q3}+i\beta_n'^3R_{M3}}{D_jl_xf_j(\alpha_M',\beta_n')} & \frac{R_{Q3}+i\beta_n'^3R_{M3}}{D_jl_xf_j(\alpha_M',\beta_n')} & \cdots & \frac{R_{Q3}+i\beta_n'^3R_{M3}}{D_jl_xf_j(\alpha_M',\beta_n')}\end{bmatrix}_{M\times N} \tag{A.7}$$

$$T_{11,2}=\begin{bmatrix}\lambda^{11,2}_{M1,1} & & & \\ & \lambda^{11,2}_{M2,1} & & \\ & & \ddots & \\ & & & \lambda^{11,2}_{MN,1}\end{bmatrix}_{MN\times MN} \tag{A.8}$$

$$T_{22,2}=\begin{bmatrix}\lambda^{11,2}_{M1,2} & & & \\ & \lambda^{11,2}_{M2,2} & & \\ & & \ddots & \\ & & & \lambda^{11,2}_{MN,2}\end{bmatrix}_{MN\times MN} \tag{A.9}$$

$$\lambda^{11,3}_{Mn,j}=\begin{bmatrix}\frac{i\alpha_1\alpha_1'\beta_n'R_{T3}}{D_jl_xf_j(\alpha_1',\beta_n')} & \frac{i\alpha_2\alpha_1'\beta_n'R_{T3}}{D_jl_xf_j(\alpha_1',\beta_n')} & \cdots & \frac{i\alpha_M\alpha_1'\beta_n'R_{T3}}{D_jl_xf_j(\alpha_1',\beta_n')}\\ \frac{i\alpha_1\alpha_2'\beta_n'R_{T3}}{D_jl_xf_j(\alpha_2',\beta_n')} & \frac{i\alpha_2\alpha_2'\beta_n'R_{T3}}{D_jl_xf_j(\alpha_2',\beta_n')} & \cdots & \frac{i\alpha_M\alpha_2'\beta_n'R_{T3}}{D_jl_xf_j(\alpha_2',\beta_n')}\\ \vdots & \vdots & \ddots & \vdots\\ \frac{i\alpha_1\alpha_M'\beta_n'R_{T3}}{D_jl_xf_j(\alpha_M',\beta_n')} & \frac{i\alpha_2\alpha_M'\beta_n'R_{T3}}{D_jl_xf_j(\alpha_M',\beta_n')} & \cdots & \frac{i\alpha_M\alpha_M'\beta_n'R_{T3}}{D_jl_xf_j(\alpha_M',\beta_n')}\end{bmatrix}_{M\times N} \tag{A.10}$$

$$T_{11,3}=\begin{bmatrix}\lambda^{11,3}_{M1,1} & & & \\ & \lambda^{11,3}_{M2,1} & & \\ & & \ddots & \\ & & & \lambda^{11,3}_{MN,1}\end{bmatrix}_{MN\times MN} \tag{A.11}$$

$$T_{22,3}=\begin{bmatrix}\lambda^{11,3}_{M1,2} & & & \\ & \lambda^{11,3}_{M2,2} & & \\ & & \ddots & \\ & & & \lambda^{11,3}_{MN,2}\end{bmatrix}_{MN\times MN} \tag{A.12}$$

$$\lambda^{11,4}_{Mn,j}=\begin{bmatrix}\frac{R_{Q1}+i\alpha_1'^3R_{M1}}{D_jl_yf_j(\alpha_1',\beta_n')} & & & \\ & \frac{R_{Q1}+i\alpha_2'^3R_{M1}}{D_jl_yf_j(\alpha_2',\beta_n')} & & \\ & & \ddots & \\ & & & \frac{R_{Q1}+i\alpha_M'^3R_{M1}}{D_jl_yf_j(\alpha_M',\beta_n')}\end{bmatrix}_{M\times N} \tag{A.13}$$

$$T_{11,4}=\begin{bmatrix}\lambda^{11,4}_{M1,1} & \lambda^{11,4}_{M1,1} & \cdots & \lambda^{11,4}_{M1,1}\\ \lambda^{11,4}_{M2,1} & \lambda^{11,4}_{M2,1} & \cdots & \lambda^{11,4}_{M2,1}\\ \vdots & \vdots & \ddots & \vdots\\ \lambda^{11,4}_{MN,1} & \lambda^{11,4}_{MN,1} & \cdots & \lambda^{11,4}_{MN,1}\end{bmatrix}_{MN\times MN} \tag{A.14}$$

$$T_{22,4}=\begin{bmatrix}\lambda^{11,4}_{M1,2} & \lambda^{11,4}_{M1,2} & \cdots & \lambda^{11,4}_{M1,2}\\ \lambda^{11,4}_{M2,2} & \lambda^{11,4}_{M2,2} & \cdots & \lambda^{11,4}_{M2,2}\\ \vdots & \vdots & \ddots & \vdots\\ \lambda^{11,4}_{MN,2} & \lambda^{11,4}_{MN,2} & \cdots & \lambda^{11,4}_{MN,2}\end{bmatrix}_{MN\times MN} \tag{A.15}$$

$$\lambda^{11,5}_{Mn',jn}=\begin{bmatrix}\frac{i\alpha_1'\beta_{n'}'\beta_nR_{T1}}{D_jl_yf_j(\alpha_1',\beta_{n'}')} & & & \\ & \frac{i\alpha_2'\beta_{n'}'\beta_nR_{T1}}{D_jl_yf_j(\alpha_2',\beta_{n'}')} & & \\ & & \ddots & \\ & & & \frac{i\alpha_M'\beta_{n'}'\beta_nR_{T1}}{D_jl_yf_j(\alpha_M',\beta_{n'}')}\end{bmatrix}_{M\times N} \tag{A.16}$$

$$T_{11,5}=\begin{bmatrix}\lambda^{11,5}_{M1,11} & \lambda^{11,5}_{M1,12} & \cdots & \lambda^{11,5}_{M1,1N}\\ \lambda^{11,5}_{M2,11} & \lambda^{11,5}_{M2,12} & \cdots & \lambda^{11,5}_{M2,1N}\\ \vdots & \vdots & \ddots & \vdots\\ \lambda^{11,5}_{MN,11} & \lambda^{11,5}_{MN,12} & \cdots & \lambda^{11,5}_{MN,1N}\end{bmatrix}_{MN\times MN} \tag{A.17}$$

$$T_{22,5}=\begin{bmatrix}\lambda^{11,5}_{M1,21} & \lambda^{11,5}_{M1,22} & \cdots & \lambda^{11,5}_{M1,2N}\\ \lambda^{11,5}_{M2,21} & \lambda^{11,5}_{M2,22} & \cdots & \lambda^{11,5}_{M2,2N}\\ \vdots & \vdots & \ddots & \vdots\\ \lambda^{11,5}_{MN,21} & \lambda^{11,5}_{MN,22} & \cdots & \lambda^{11,5}_{MN,2N}\end{bmatrix}_{MN\times MN} \tag{A.18}$$

$$\lambda^{12,1}_{Mn,j}=-\begin{bmatrix}\frac{R_{Q4}+i\beta_n'^3R_{M4}}{D_jl_xf_j(\alpha_1',\beta_n')} & \frac{R_{Q4}+i\beta_n'^3R_{M4}}{D_jl_xf_j(\alpha_1',\beta_n')} & \cdots & \frac{R_{Q4}+i\beta_n'^3R_{M4}}{D_jl_xf_j(\alpha_1',\beta_n')}\\ \frac{R_{Q4}+i\beta_n'^3R_{M4}}{D_jl_xf_j(\alpha_2',\beta_n')} & \frac{R_{Q4}+i\beta_n'^3R_{M4}}{D_jl_xf_j(\alpha_2',\beta_n')} & \cdots & \frac{R_{Q4}+i\beta_n'^3R_{M4}}{D_jl_xf_j(\alpha_2',\beta_n')}\\ \vdots & \vdots & \ddots & \vdots\\ \frac{R_{Q4}+i\beta_n'^3R_{M4}}{D_jl_xf_j(\alpha_M',\beta_n')} & \frac{R_{Q4}+i\beta_n'^3R_{M4}}{D_jl_xf_j(\alpha_M',\beta_n')} & \cdots & \frac{R_{Q4}+i\beta_n'^3R_{M4}}{D_jl_xf_j(\alpha_M',\beta_n')}\end{bmatrix}_{M\times N} \tag{A.19}$$

$$T_{12,1}=\begin{bmatrix}\lambda^{12,1}_{M1,1} & & & \\ & \lambda^{12,1}_{M2,1} & & \\ & & \ddots & \\ & & & \lambda^{12,1}_{MN,1}\end{bmatrix}_{MN\times MN} \tag{A.20}$$

$$T_{21,1}=\begin{bmatrix}\lambda^{12,1}_{M1,2} & & & \\ & \lambda^{12,1}_{M2,2} & & \\ & & \ddots & \\ & & & \lambda^{12,1}_{MN,2}\end{bmatrix}_{MN\times MN} \tag{A.21}$$

$$\lambda^{12,2}_{Mn,j}=-\begin{bmatrix}\frac{i\alpha_1\alpha_1'\beta_n'R_{T4}}{D_jl_xf_j(\alpha_1',\beta_n')} & \frac{i\alpha_2\alpha_1'\beta_n'R_{T4}}{D_jl_xf_j(\alpha_1',\beta_n')} & \cdots & \frac{i\alpha_M\alpha_1'\beta_n'R_{T4}}{D_jl_xf_j(\alpha_1',\beta_n')}\\ \frac{i\alpha_1\alpha_2'\beta_n'R_{T4}}{D_jl_xf_j(\alpha_2',\beta_n')} & \frac{i\alpha_2\alpha_2'\beta_n'R_{T4}}{D_jl_xf_j(\alpha_2',\beta_n')} & \cdots & \frac{i\alpha_M\alpha_2'\beta_n'R_{T4}}{D_jl_xf_j(\alpha_2',\beta_n')}\\ \vdots & \vdots & \ddots & \vdots\\ \frac{i\alpha_1\alpha_M'\beta_n'R_{T4}}{D_jl_xf_j(\alpha_M',\beta_n')} & \frac{i\alpha_2\alpha_M'\beta_n'R_{T4}}{D_jl_xf_j(\alpha_M',\beta_n')} & \cdots & \frac{i\alpha_M\alpha_M'\beta_n'R_{T4}}{D_jl_xf_j(\alpha_M',\beta_n')}\end{bmatrix}_{M\times N} \tag{A.22}$$

$$T_{12,2}=\begin{bmatrix}\lambda^{12,2}_{M1,1} & & & \\ & \lambda^{12,2}_{M2,1} & & \\ & & \ddots & \\ & & & \lambda^{12,2}_{MN,1}\end{bmatrix}_{MN\times MN} \tag{A.23}$$

$$T_{21,2}=\begin{bmatrix}\lambda^{12,2}_{M1,2} & & & \\ & \lambda^{12,2}_{M2,2} & & \\ & & \ddots & \\ & & & \lambda^{12,2}_{MN,2}\end{bmatrix}_{MN\times MN} \tag{A.24}$$

$$\lambda^{12,3}_{Mn,j} = -\begin{bmatrix} \frac{R_{Q2}+i\alpha_1'^3 R_{M2}}{D_j l_y f_j(\alpha_1',\beta_n')} & & & \\ & \frac{R_{Q2}+i\alpha_2'^3 R_{M2}}{D_j l_y f_j(\alpha_2',\beta_n')} & & \\ & & \ddots & \\ & & & \frac{R_{Q2}+i\alpha_M'^3 R_{M2}}{D_j l_y f_j(\alpha_M',\beta_n')} \end{bmatrix}_{M\times N} \tag{A.25}$$

$$T_{12,3} = \begin{bmatrix} \lambda^{12,3}_{M1,1} & \lambda^{12,3}_{M1,1} & \cdots & \lambda^{12,3}_{M1,1} \\ \lambda^{12,3}_{M2,1} & \lambda^{12,3}_{M2,1} & \cdots & \lambda^{12,3}_{M2,1} \\ \vdots & \vdots & \ddots & \vdots \\ \lambda^{12,3}_{MN,1} & \lambda^{12,3}_{MN,1} & \cdots & \lambda^{12,3}_{MN,1} \end{bmatrix}_{MN\times MN} \tag{A.26}$$

$$T_{21,3} = \begin{bmatrix} \lambda^{12,3}_{M1,2} & \lambda^{12,3}_{M1,2} & \cdots & \lambda^{12,3}_{M1,2} \\ \lambda^{12,3}_{M2,2} & \lambda^{12,3}_{M2,2} & \cdots & \lambda^{12,3}_{M2,2} \\ \vdots & \vdots & \ddots & \vdots \\ \lambda^{12,3}_{MN,2} & \lambda^{12,3}_{MN,2} & \cdots & \lambda^{12,3}_{MN,2} \end{bmatrix}_{MN\times MN} \tag{A.27}$$

$$\lambda^{12,4}_{Mn'jn} = -\begin{bmatrix} \frac{i\alpha_1'\beta_{n'}'\beta_n R_{T2}}{D_j l_y f_j(\alpha_1',\beta_{n'}')} & & & \\ & \frac{i\alpha_2'\beta_{n'}'\beta_n R_{T2}}{D_j l_y f_j(\alpha_2',\beta_{n'}')} & & \\ & & \ddots & \\ & & & \frac{i\alpha_M'\beta_{n'}'\beta_n R_{T2}}{D_j l_y f_j(\alpha_M',\beta_{n'}')} \end{bmatrix}_{M\times N} \tag{A.28}$$

$$T_{12,4} = \begin{bmatrix} \lambda^{12,4}_{M1,11} & \lambda^{12,4}_{M1,12} & \cdots & \lambda^{12,4}_{M1,1N} \\ \lambda^{12,4}_{M2,11} & \lambda^{12,4}_{M2,12} & \cdots & \lambda^{12,4}_{M2,1N} \\ \vdots & \vdots & \ddots & \vdots \\ \lambda^{12,4}_{MN,11} & \lambda^{12,4}_{MN,12} & \cdots & \lambda^{12,4}_{MN,1N} \end{bmatrix}_{MN\times MN} \tag{A.29}$$

$$T_{21,4} = \begin{bmatrix} \lambda^{12,4}_{M1,21} & \lambda^{12,4}_{M1,22} & \cdots & \lambda^{12,4}_{M1,2N} \\ \lambda^{12,4}_{M2,21} & \lambda^{12,4}_{M2,22} & \cdots & \lambda^{12,4}_{M2,2N} \\ \vdots & \vdots & \ddots & \vdots \\ \lambda^{12,4}_{MN,21} & \lambda^{12,4}_{MN,22} & \cdots & \lambda^{12,4}_{MN,2N} \end{bmatrix}_{MN\times MN} \tag{A.30}$$

Employing the definition of the sub-matrices presented above, one obtains:

$$\begin{aligned} T_{11} &= T_{11,1} + T_{11,2} + T_{11,3} + T_{11,4} + T_{11,5}, \\ T_{22} &= T_{22,1} + T_{22,2} + T_{22,3} + T_{22,4} + T_{22,5} \end{aligned} \tag{A.31}$$

$$\begin{aligned} T_{12} &= T_{12,1} + T_{12,2} + T_{12,3} + T_{12,4}, \\ T_{21} &= T_{21,1} + T_{21,2} + T_{21,3} + T_{21,4} \end{aligned} \tag{A.32}$$

References

[1] Ichchou MN, Berthaut J, Collet M. Multi-mode wave propagation in ribbed plates. Part I: Wavenumber-space characteristics. Int J Solids Struct 2008;45(5):1179–95.

[2] Ichchou MN, Berthaut J, Collet M. Multi-mode wave propagation in ribbed plates. Part II: Predictions and comparisons. Int J Solids Struct 2008;45(5):1196–216.

[3] Mace BR. Periodically stiffened fluid-loaded plates. I: Response to convected harmonic pressure and free wave propagation. J Sound Vib 1980;73(4):473–86.

[4] Mace BR. Periodically stiffened fluid-loaded plates. II: Response to line and point forces. J Sound Vib 1980;73(4):487–504.

[5] Mace BR. Sound radiation from fluid loaded orthogonally stiffened plates. J Sound Vib 1981;79(3):439–52.

[6] Mace BR. The vibration of plates on two-dimensionally periodic point supports. J Sound Vib 1996;192(3):629–43.

[7] Lee JH, Kim J. Analysis of sound transmission through periodically stiffened panels by space-harmonic expansion method. J Sound Vib 2002;251(2):349–66.

[8] Yin XW, Gu XJ, Cui HF, Shen RY. Acoustic radiation from a laminated composite plate reinforced by doubly periodic parallel stiffeners. J Sound Vib 2007;306(3–5):877–89.

[9] Xin FX, Lu TJ, Chen CQ. Vibroacoustic behavior of clamp mounted double-panel partition with enclosure air cavity. J Acoust Soc Am 2008;124(6):3604–12.

[10] Xin FX, Lu TJ, Chen C. Sound transmission through lightweight all-metallic sandwich panels with corrugated cores. Multi-functional materials and structures, parts 1 and 2. Adv Mater Res 2008;47–50:57–60.

[11] Maxit L. Wavenumber space and physical space responses of a periodically ribbed plate to a point drive: a discrete approach. Appl Acoust 2009;70(4):563–78.

[12] Xin FX, Lu TJ. Analytical and experimental investigation on transmission loss of clamped double panels: Implication of boundary effects. J Acoust Soc Am 2009;125(3):1506–17.

[13] Xin FX, Lu TJ, Chen CQ. Dynamic response and acoustic radiation of double-leaf metallic panel partition under sound excitation. Comput Mater Sci 2009;46(3):728–32.

[14] Xin FX, Lu TJ, Chen CQ. External mean flow influence on noise transmission through double-leaf aeroelastic plates. AIAA J 2009;47(8):1939–51.

[15] Takahashi D. Sound radiation from periodically connected double-plate structures. J Sound Vib 1983;90(4):541–57.

[16] Fahy FJ, Lindqvist E. Wave propagation in damped, stiffened structures characteristic of ship construction. J Sound Vib 1976;45(1):115–38.

[17] Mead DJ. Plates with regular stiffening in acoustic media: vibration and radiation. J Acoust Soc Am 1990;88(1):391–401.

[18] Xin FX, Lu TJ, Chen CQ. Sound transmission through simply supported finite double-panel partitions with enclosed air cavity. ASME J Vib Acoust 2010;132(1):1–11. 011008.

[19] Xin FX, Lu TJ. Sound radiation of orthogonally rib-stiffened sandwich structures with cavity absorption. Compos Sci Technol 2010;70(15):2198–206.

[20] Xin FX, Lu TJ. Analytical modeling of sound transmission across finite aeroelastic panels in convected fluids. J Acoust Soc Am 2010;128(3):1097–107.

[21] Mead DJ, Pujara KK. Space-harmonic analysis of periodically supported beams: response to convected random loading. J Sound Vib 1971;14(4):525–32.

[22] Mead DJ, Yaman Y. The harmonic response of uniform beams on multiple linear supports: a flexural wave analysis. J Sound Vib 1990;141(3):465–84.

[23] Mead DJ. Free wave propagation in periodically supported, infinite beams. J Sound Vib 1970;11(2):181–97.

[24] Mead DJ. Wave propagation in continuous periodic structures: research contributions from Southampton, 1964–1995. J Sound Vib 1996;190(3):495–524.

[25] Rumerman ML. Vibration and wave propagation in ribbed plates. J Acoust Soc Am 1975;57(2):370–3.

[26] Mead DJ, Mallik AK. An approximate theory for the sound radiated from a periodic line-supported plate. J Sound Vib 1978;61(3):315–26.

[27] Mead DJ, Parthan S. Free wave propagation in two-dimensional periodic plates. J Sound Vib 1979;64(3):325–48.

[28] Mace BR. Sound radiation from a plate reinforced by two sets of parallel stiffeners. J Sound Vib 1980;71(3):435–41.

[29] Cray BA. Acoustic radiation from periodic and sectionally aperiodic rib-stiffened plates. J Acoust Soc Am 1994;95(1):256–64.

[30] Wang J, Lu TJ, Woodhouse J, Langley RS, et al. Sound transmission through lightweight double-leaf partitions: theoretical modelling. J Sound Vib 2005;286(4–5):817–47.

[31] Crighton DG. Transmission of energy down periodically ribbed elastic structures under fluid loading. Proc R Soc Lond A 1984;394(1807):405–36.

[32] Spivack M. Wave propagation in finite periodically ribbed structures with fluid loading. Proc R Soc Lond A 1991;435(1895):615–34.

[33] Cooper AJ, Crighton DG. Transmission of energy down periodically ribbed elastic structures under fluid loading: spatial periodicity in the pass bands. Proc R Soc Lond A 1998;454(1979):2893–909.

[34] Cooper AJ, Crighton DG. Transmission of energy down periodically ribbed elastic structures under fluid loading: algebraic decay in the stop bands. Proc R Soc Lond A 1998;454(1973):1337–55.

[35] Kohno H, Bathe K-J, Wright JC. A finite element procedure for multiscale wave equations with application to plasma waves. Comput Struct 2010;88(1–2):87–94.

[36] Xin FX, Lu TJ. Analytical modeling of fluid loaded orthogonally rib-stiffened sandwich structures: sound transmission. J Mech Phys Solids 2010;58(9):1374–96.

[37] Morse PM, Ingard KU. Theoretical acoustics. New York: McGraw-Hill; 1968.

[38] Castanier MP, Pierre C. Lyapunov exponents and localization phenomena in multi-coupled nearly periodic systems. J Sound Vib 1995;183(3):493–515.

[39] Li FM, Wang YS, Hu C, Huang WH. Localization of elastic waves in periodic rib-stiffened rectangular plates under axial compressive load. J Sound Vib 2005;281(1–2):261–73.